NASA CONTRACTOR REPORT

NASA CR-681

PASSIVE INFRARED ACQUISITION AND TRACKING SYSTEM ANALYSIS

TASK II

by John G. Braithwaite

Prepared by
UNIVERSITY OF MICHIGAN
Ann Arbor, Mich.
for Goddard Space Flight Center

NATIONAL AERONAUTICS AND SPACE ADMINISTRATION • WASHINGTON, D. C. • JANUARY 1967

PASSIVE INFRARED ACQUISITION AND TRACKING SYSTEM ANALYSIS

TASK II

By John G. Braithwaite

Prepared under Contract No. NAS 5-9585 by
UNIVERSITY OF MICHIGAN
Ann Arbor, Mich.

for Goddard Space Flight Center

NATIONAL AERONAUTICS AND SPACE ADMINISTRATION

For sale by the Clearinghouse for Federal Scientific and Technical Information
Springfield, Virginia 22151 – Price $2.00

ABSTRACT

When the Apollo Command Module returning from a lunar mission enters the earth's atmosphere, considerable radiant energy is emitted from the surface of the module and from the shocked air and wake surrounding the module. Detection of this radiation by an acquisition and tracking system is complicated by background radiation, which is defined. The spectral properties of both source and background radiation are analyzed to determine the optimum wavelength region for operating an optical acquisition and tracking system. The determination of the spectral properties of the target by a parallel Task I report is cited.

The target spectral intensity shows a maximum and the background spectral radiance a minimum in the 3- to 5-μ wavelength band, from which it is demonstrated that this is the optimum operational wavelength region. From an analysis of the literature on atmospheric transmission the conclusion is drawn that the upper atmosphere will be very transparent over most of this wavelength range.

CONTENTS

Abstract iii
List of Figures vi
List of Tables vii
1. Introduction 1
2. Spurious Signals and Noise 1
3. Target Characteristics 2
4. Background Spectra 4
5. Choosing the Optimum Wavelength Region 6
Appendix I: Background Quantum Noise Considerations 8
Appendix II: Atmospheric Transmission from 2- to 5-μ for Slant Paths from 35,000 ft to the Limit of the Atmosphere 9
References 25

FIGURES

1. Surface and Gas Cap Radiation Histories for the Apollo Vehicle on an Undershoot Trajectory: 1.8-2.7 μ, 3.3-5.0 μ, and 8.0-12.0 μ; Forward Aspect 3
2. Surface and Gas Cap Radiation Histories and the Apollo Vehicle on an Overshoot Trajectory: 1.8-2.7 μ, 3.3-5.0 μ, and 8.0-12.0 μ; Forward Aspect 3
3. An Idealized Spectral Radiance of the Sun, Emitting Atmosphere, Sunlit Cloud, and Sunlight-Scattering Clear Sky 5
4. The Spectral Radiance of a Clear Sky for Angles of Elevation Above the Horizon in the Sequence 0^{o}, 1.8^{o}, 3.6^{o}, 7.2^{o}, 14.5^{o}, 30^{o}, 90^{o} 5
5. The Spectral Radiance of a Clear Sky, Showing the Elevation-Angle Dependence of the Scattered Radiation 5
6. A Section of the Solar Spectrum as Observed from a Canberra Aircraft . . . 10
7. Solar Spectral Irradiance in the 2.8-μ Region at Various Altitudes 12
8. Transmittance Determined from Solar Radiation Measurements 13
9. Yearly Averages of Transmission Versus Wavelength 14
10. Transmission Versus Wavelength 16
11. Transmission Versus Wavelength 16
12. Transmission Versus Wavelength 16
13. Transmission Versus Wavelength 16
14. Observed Spectral Transmission of the Atmosphere at Various Altitudes for the Region 2800 cm^{-1} to 3300 cm^{-1} 17
15. Observed Spectral Transmission of the Atmosphere at Various Altitudes for the Region 3200 cm^{-1} to 4200 cm^{-1} 17
16. Observed Spectral Transmission of the Atmosphere at Various Altitudes for the Region 4100 cm^{-1} to 5100 cm^{-1}. 17
17. Transmission Versus Wavelength 19
18. Theoretical and Observed Spectral Transmission of the Atmosphere at 15 km Altitude for the Region from 4.0 μ to 4.65 μ 20
19. Theoretical and Observed Spectral Transmission of the Atmosphere at 25 km Altitude for the Region from 4.0 μ to 4.65 μ 20
20. Theoretical and Observed Spectral Transmission of the Atmosphere at 30 km Altitude for the Region from 4.0 μ to 4.65 μ 20
21. Solar Spectra: 2.4—3.6 μ 21
22. Solar Spectra: 1.7—2.9 μ 21
23. Transmission Versus Wavelength Determined from Reduced Solar Spectra. 23
24. Composite Transmission Spectra 24

TABLES

I. Wavelength Dependence of Target Intensity, Background Radiance, and Detector N.E.P. 7

II. Balloon Flight, 17 January 1963 18

FIRST PROGRESS REPORT FOR PASSIVE INFRARED ACQUISITION AND TRACKING SYSTEM ANALYSIS TASK II

1 INTRODUCTION

The work statement for Task II requires the contractor to determine the optimum wavelength for operation of an Apollo acquisition and tracking system during earth reentry. A complete analysis of this problem would be a major undertaking if it were necessary to determine the spatial and spectral characteristics of all possible background situations and to analyze the performance of all scanning systems against each background for each wavelength range. Fortunately, it is possible to choose the 3- to 5-μ wavelength range on the basis of relatively simple but conclusive arguments. In addition to these arguments, the results of a study of the atmospheric transmission conditions likely to be met in this wavelength range—a study based on extensive examination of the literature—are presented in detail in appendix II.

2 SPURIOUS SIGNALS AND NOISE

Radiant backgrounds interfere with detection of radiant targets in two distinct ways. First, discontinuities and gradients in the background may give rise to signals which may be mistaken for target signals. Such unwanted signals are often called background noise, though background signals or spurious signals are better names. Spatial and spectral filtering techniques of greater or lesser elaboration have been used to discriminate against background signals. In general, the selection of an optimum spectral region for operating a detector cannot be made independently of the selection of a spatial filtering technique. However, it would be possible to make an independent choice if the spatial spectrum of the background were independent of wavelength except for a wavelength independent multiplicative constant. In this instance a given spatial discrimination technique would give equivalent improvement when used at any wavelength range. As is shown in section 4, blue sky and clouds, the two backgrounds of importance, have surprisingly similar spectra. Thus we can choose the optimum wavelength region for discriminating against background signals without consideration of spatial effects if we select the region in which target radiant intensity to background radiance is a maximum.

Second, background radiation interferes with the detection process through quantum effects inherent in the radiation stream and the quantum nature of the detection process. The noise

voltage associated with these effects will be proportional to the square root of the total effective photon flux falling on the detector. A simple analysis of this effect is given in appendix I. As can be seen from the final equation of that appendix, the relation is not linear with J and N (where J is the target radiant intensity and N is the background radiance). Fortunately, as is later explained, the 3- to 5-μ region gives both a maximum in qJ (where q is the quantum efficiency of the detector) and a minimum in N/J, so that this is clearly the optimum wavelength range for maximizing the S/N given by this equation.

The problem of selecting the optimum wavelength region is simplified by considering the N and J effects and detector noise or quantum efficiency separately in section 5 following the discussions of target and background spectra in sections 3 and 4. It should be noticed that this is a fortuitous consequence of the fact that the 3- to 5-μ spectral region is optimum with regard to both kinds of background effect and target-to-detector noise (for state-of-the-art detectors appropriate to the various wavelength ranges). If this were not so, more complicated analyses would be necessary to choose the best wavelength range.

3
TARGET CHARACTERISTICS

The spectral radiance of the reentering Apollo vehicle as a function of time, aspect, and wavelength is discussed in the Task I report [1]. This report shows that during the skip period: (1) the target radiance will be at a minimum for all wavelengths; (2) for both undershoot and overshoot conditions there will be a rather flat maximum in the target spectrum centered at about 4 μ (perhaps at slightly longer wavelengths for the overshoot trajectory); and (3) the visible radiance from the shock cap virtually disappears. Since the reentering Apollo vehicle must be tracked continuously through the skip period, it is clear that the spectrum of the target at this time is the one to be considered. Inspection of the curves derived by Task I, the two most important of which are reproduced here as figures 1 and 2, shows in fact that from the point of view of target intensity, the only serious competitor to the 3.3- to 5-μ band is the 8- to 12-μ band.

At the start of reentry and following skip periods, the intensity rises rapidly and nearly simultaneously in all wavelength bands. Thus, the choice of wavelength band will not have an important effect on the time of first acquisition, which should, of course, occur as early as possible. During the skip period the intensity in the wavelength region below 3 μ falls much more rapidly and much further than the intensity at longer wavelengths (figs. 1 and 2). Since

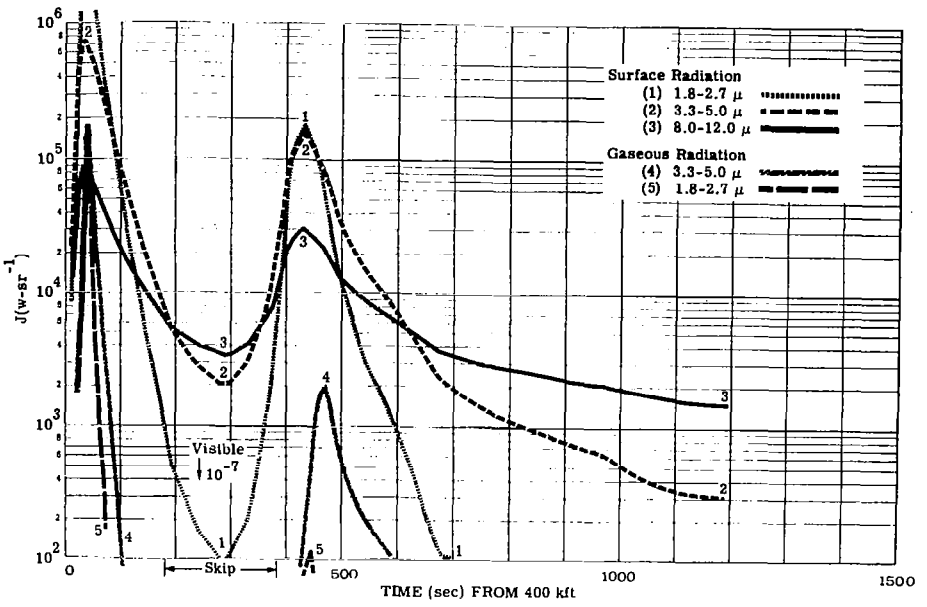

FIGURE 1. SURFACE AND GAS CAP RADIATION HISTORIES FOR THE APOLLO VEHICLE ON AN UNDERSHOOT TRAJECTORY: 1.8-2.7 μ, 3.3-5.0 μ, and 8.0-12.0 μ; FORWARD ASPECT [1]

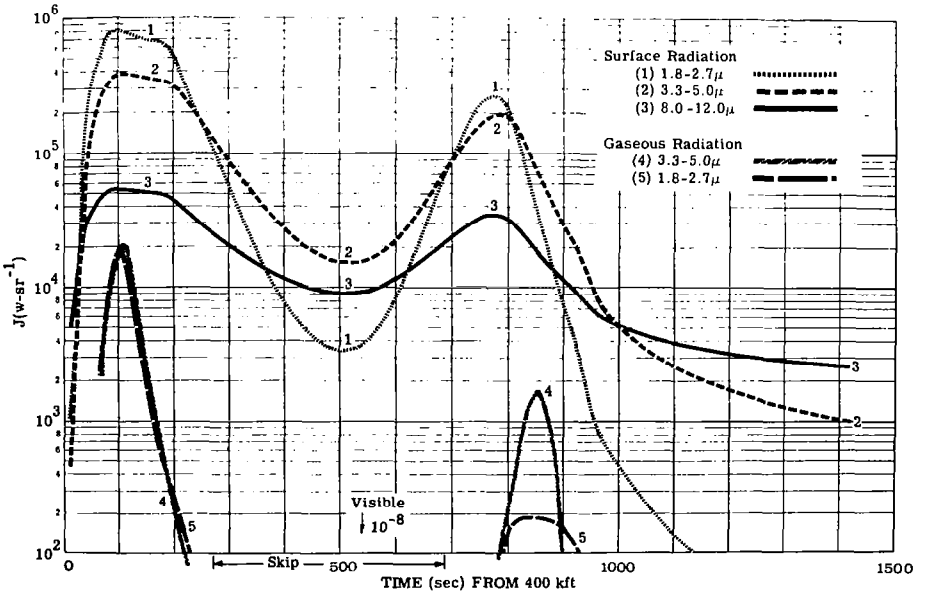

FIGURE 2. SURFACE AND GAS CAP RADIATION HISTORIES FOR THE APOLLO VEHICLE ON AN OVERSHOOT TRAJECTORY: 1.8-2.7 μ, 3.3-5.0 μ, and 8.0-12.0 μ; FORWARD ASPECT [1]

the same effect holds for the final descent, selecting one of the longer wavelength bands will also ensure that the target can be tracked to the lowest possible altitude.

The Task I report also gives much data on the aspect dependence of the radiation as a function of time and wavelength band. While figures 1 and 2 refer specifically to forward aspect radiation, the Task I report shows that the radiation is similarly reduced in all wavelength bands for other aspects, especially for the rear aspect. However, the effect is much more marked at the shorter wavelengths. In particular the decrease in the 1.8- to 2.7-μ band during the skip period is about one order of magnitude more than that shown by the longer wavelength bands.

Thus, consideration of target spectral radiance clearly makes the 3.3- to 5-μ band the optimum region with the 8- to 12-μ band a second choice.

4
BACKGROUND SPECTRA

The high altitude background radiances with which we are concerned are composed of scattered and reflected sunlight and the self-emission of gas molecules and particulate matter such as the water droplets and ice crystals of clouds. (The stars, though self-luminous, have spectra so similar to the sun's that they need not be considered spectrally. It can be shown that a few of the brightest stars will be equivalent to the weakest targets in the 3-μ wavelength region.) There is a minimum in the composite spectrum of these sources at about 3 to 5 μ, as shown in the ground-based measurements of Bell et al. [2], three of whose diagrams are reproduced as figures 3, 4, and 5. At high altitudes both scattered and emitted radiation will be reduced because of fewer scattering centers and the lower temperature of the emitting material. However, the minimum in the 3- to 5-μ region will remain. Also note that the presence of clouds will have little effect on this conclusion (fig. 3), though it will, of course, be impossible to see the target through clouds unless they are very thin. At the longer wavelengths where emission is important, clouds are essentially blackbodies, whereas clear sky radiates only at those wavelengths where atmospheric absorption occurs. While the 3.4- to 4.1-μ region is highly transmitting, figure 4 suggests that the 10-μ atmospheric transmission is less satisfactory in this respect, particularly at the lower elevation angles that are quite important in the Apollo acquisition and tracking system.

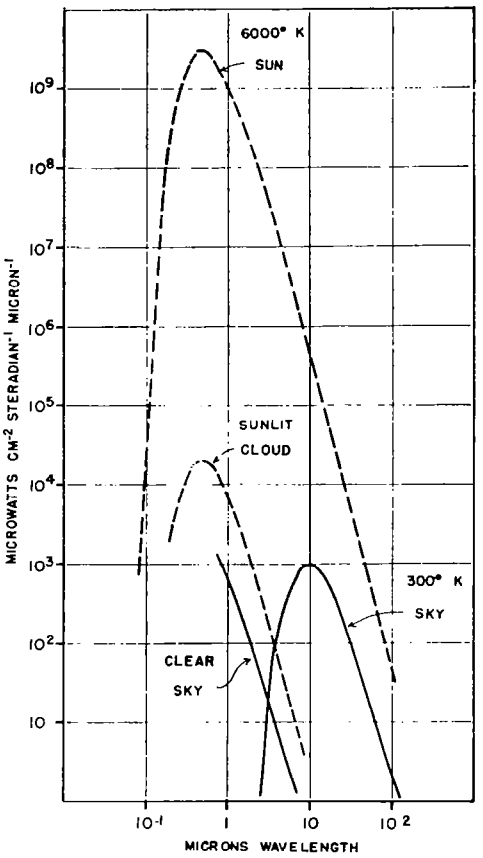

FIGURE 3. AN IDEALIZED SPECTRAL RADIANCE OF THE SUN, EMITTING ATMOSPHERE, SUNLIT CLOUD, AND SUNLIGHT-SCATTERING CLEAR SKY (BELL) [2]

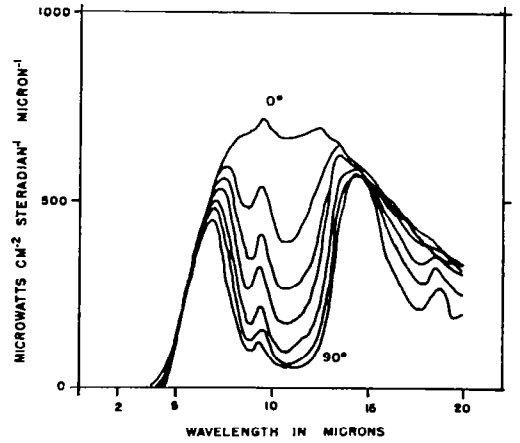

FIGURE 4. THE SPECTRAL RADIANCE OF A CLEAR SKY FOR ANGLES OF ELEVATION ABOVE THE HORIZON IN THE SEQUENCE 0°, 1.8°, 3.6°, 7.2°, 14.5°, 30°, 90°. Measured at the Elk Park station, Colorado, on a September night. Altitude = 11,000 ft. Ambient temperature = 8°C. (BELL) [2]

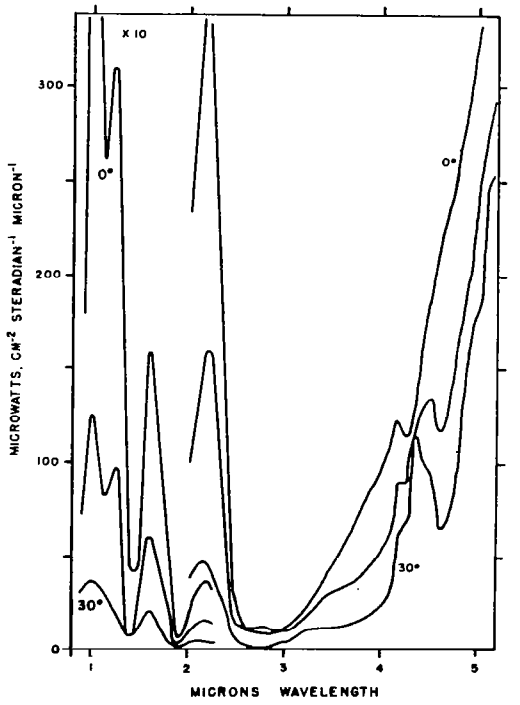

FIGURE 5. THE SPECTRAL RADIANCE OF A CLEAR SKY, SHOWING THE ELEVATION-ANGLE DEPENDENCE OF THE SCATTERED RADIATION. Measured at Colorado Springs, near noon during September. Elevation angles = 0° (highest curve), 7.2°, and 30° (lowest curve). The radiance values for the short-wave portion are ten times larger than the ordinate scale shown. (BELL) [2]

5
CHOOSING THE OPTIMUM WAVELENGTH REGION

Sections 3 and 4 have shown that the 3- to 5-μ region provides both the highest spectral intensity of the target during the critical skip phase of reentry and the lowest background spectral radiance. Thus, if detector performance is ignored, it is clear that the 3- to 5-μ atmospheric windows is the preferred spectral region. Detector performance considerations indeed do not alter this decision. Table I shows that while detector performance in terms of noise equivalent power (NEP) is much better in the shorter wavelength bands, the increase in target intensity with wavelength more than offsets the decrease in NEP, as shown by the ratio of J/NEP. As explained in section 3, the advantage of the 3.3- to 5-μ range over the 1.8- to 2.7-μ range becomes even more pronounced when aspects other than the forward are considered.

Detectors with fast response times (1 μsec) are available for all wavelengths ranges, those used in the three infrared bands requiring cooling to cryogenic temperatures. However, InSb detectors using the 3.3- to 5.0-μ region operate at a temperature (77^{o}K) much more readily produced than the cooling temperatures (< 35^{o}K) required by Ge:Hg detectors to operate in the 8- to 12-μ region.

Thus, relatively simple but conclusive arguments show that the 3.3- to 5-μ wavelength region is optimum for use in the Apollo Infrared Acquisition and Tracking System, both signal-to-detector noise and signal-to-background noise having been considered. Furthermore, this conclusion is not vitiated by atmospheric transmission considerations.

A search of the literature was conducted to determine in detail the transmission characteristics of relevant atmospheric paths in this wavelength range. An account of this study is given in appendix II, from which it appears that the atmospheric path above 35,000 ft will be highly transparent outside the limits of the 3.3- and 4.3-μ absorption bands, over the 2.9- to 4.5-μ region. There are strong indications that the long wavelength limit can be extended to at least 4.9 μ, and that these findings hold for zenith angles from zero to almost 90^{o}.

TABLE I. WAVELENGTH DEPENDENCE OF TARGET INTENSITY, BACKGROUND RADIANCE, AND DETECTOR N.E.P.

Wavelength Range	Detector NEP(1/D*)	J_{target} ‡	$N_{background}$	J/NEP
Visible	10^{-14} †	10^{-7}	5×10^{3}	10^{7}
1.8 to 2.7 μ	2.10^{-12}	1×10^{2}	5×10^{2}	5.10^{13}
3.3 to 5 μ	2.10^{-11}	2×10^{3}	1.5×10^{2}	1.10^{14}
8 to 12 μ	5.10^{-11}	3.5×10^{2}	4.10^{3}	7.10^{13}

†This is approximately the NEP of a photomultiplier working under dark conditions. With a bright background its effective NEP will be poorer, generally much poorer.

‡At minimum intensity during skip for an undershoot trajectory and as seen from the forward aspect.

Appendix I
BACKGROUND QUANTUM NOISE CONSIDERATIONS

Our problem is a target of intensity J at a range r to be acquired and tracked against a uniform background of radiance N. Both J and N will be functions of the wavelength range chosen.

For a photoemissive detector of quantum efficiency q, the current arising from the target radiation can be expressed

$$I_s = eq\frac{\pi D^2}{4}\frac{J}{r^2}\tau k$$

where e is the electronic charge

D is the collector diameter

τ is the overall optical efficiency

k is the signal efficiency

Similarly for the current arising from the combined effect of signal and background,

$$I_b = eq(\pi/4)D^2[(J/r^2) + \theta^2 N]\tau k$$

where θ is the angular field of view. Now, the noise associated with this current is given by the well known equation:

$$I_n = \sqrt{2eI_b \Delta f}$$

where Δf is the electronic bandwidth. If $\Delta f = \frac{1}{2t}$, where t is the dwell time associated with the scanning system,

$$I_n = \sqrt{(e/t)eq(\pi/4)D^2[(J/r^2) + \theta^2 N]\tau k}$$

Thus, the signal to quantum noise is given by

$$\frac{S}{N} = \frac{I_s}{I_n} = \frac{eq(\pi/4)D^2(J/r^2)\tau k}{\sqrt{e^2(q/t)(\pi/4)D^2[(J/r^2) + \theta^2 N]\tau k}}$$

$$= \sqrt{qt(\pi/4)D^2\tau k}\ \frac{J/r^2}{\sqrt{[(J/r^2) + \theta^2 N]}}$$

(For the generation-recombination, noise-limited photovoltaic or photoconductive detector, essentially the same arguments apply, and the same result will be reached except perhaps for a constant factor.) We can rewrite the last equation

$$\frac{S}{N} = \sqrt{(\pi/4)D^2 tk}\ \sqrt{\frac{\tau q J}{1 + \theta^2 r^2 (N/J)}}$$

All the wavelength-dependent terms occur under the second root sign. Part of the argument of sections 2, 3, and 5 is, in effect, that τ, qJ (J/NEP) have maximums while N/J has a minimum in the 3- to 5-μ wavelength region.

Appendix II
ATMOSPHERIC TRANSMISSION FROM 2- TO 5-μ FOR SLANT PATHS FROM 35,000 FT TO THE LIMIT OF THE ATMOSPHERE

This appendix summarizes the available solar spectra for the 2- to 5-μ wavelength region for slant paths from 35,000 ft to the limit of the atmosphere in order to make predictions of atmospheric absorption with particular emphasis on the window regions. Unfortunately, the available data indicate that the absorption bands rather than regions of low absorption have been of primary concern to high altitude investigators. However, though the data are limited, something can be said concerning the absorption spectra for certain slant paths. Five people have reduced solar spectra to absolute transmission spectra for this spectral region, and their data are presented in this summary.

Several researchers have measured the solar spectrum to determine the nature of the absorption arising from the various atmospheric constituents [3, 4]. The first work done with ground-based instruments was only partially successful. In the stronger absorbing bands the absorption was complete, so that quantitative data could not be obtained. Houghton et al. carried out a broad program of high altitude studies of the near infrared atmospheric transmission chiefly to determine the mixing ratio of water vapor in the stratosphere [5]. The principal outcome of their study is an atlas, published in 1961, of the infrared solar spectrum from 1- to 6.5-μ observed from a Canberra aircraft at altitudes of 20,000 to 40,000 ft. A sample of the spectra is shown in figure 6. Unfortunately, the data were such that quantitative data on absorption could not be determined.

One of the first attempts to obtain absolute transmission data from solar spectra was carried out by Templin at the Naval Ordnance Laboratory, White Oak, Maryland [6]. Special attention was given to the 2.7- and 4.3-μ atmospheric absorption bands in an effort to determine the

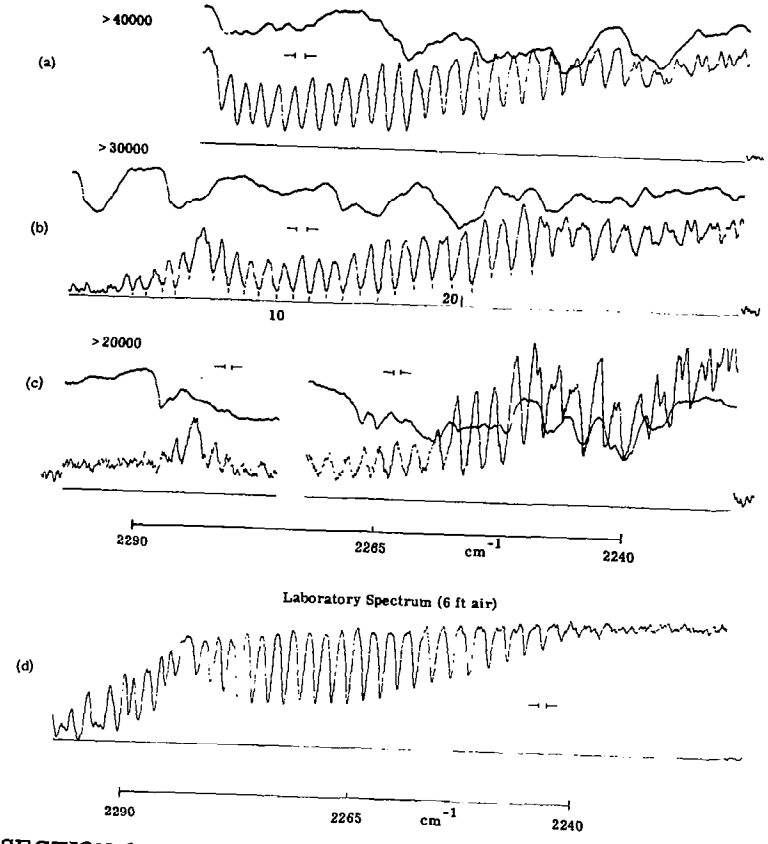

FIGURE 6. A SECTION OF THE SOLAR SPECTRUM AS OBSERVED FROM A CANBERRA AIRCRAFT (HOUGHTON) [5]

altitude at which the sun begins to appear in the center of the absorption band. In June 1955 a P2V-7 aircraft obtained spectra for altitudes up to 21,000 ft. The spectra for the 2.7-μ region are shown in figure 7. Values for absolute absorption can be obtained if the difference between the spectrum and the solar envelope is examined. Transmission values obtained from these curves are in agreement with other data, but their usefulness is limited, as the highest altitude was only 21,000 ft, and the wavelength region extended only partially into the window regions. Templin also made solar spectra measurements from Mt. Chacaltaya, Boliva at an altitude of 17,000 ft and obtained transmission values greater than 90% for the 2.3-, 3.6-, and 4.7-μ window regions [7].

John Strong of Johns Hopkins University performed some high-altitude transmission studies from a U-2 aircraft at 35,000 and 65,000 ft [8]. The data obtained were useful for determining water-vapor content and predicting the solar envelope at high altitudes, but absolute transmission values were not determined.

An extensive measurement program is being conducted by Cummings and Markle of the Canadian Armament Research and Development Establishment (CARDE) [9-14]. They are involved in a continuing investigation of the infrared solar spectrum observed from an aircraft platform. The solar spectra have been reduced to atmospheric transmission data in the 2.5- to 3.35-μ region for slant paths from space down to altitudes of 35,000 to 45,000 ft. They have also made measurements in the 3- to 5-μ region, but these data will not be reduced to transmission spectra.

A Perkin-Elmer Model 108 spectrometer utilizing a lead telluride detector and a lithium fluoride prism was flown in a CF-100 aircraft to obtain their initial data. Later the spectrometer was replaced with a model 99-G, and resolution of approximately 1 cm^{-1} was obtained. An example of their high-resolution transmission spectra is shown in figure 8. The data are presently in the form of a to-be-published atlas of transmission spectra from 2.5- to 3.35-μ. Forty-one curves of transmission vs. wavelength reduced from solar spectra taken at 35,000 ft for zenith angles ranging from 6^{o} to 91.3^{o} appear in the atlas. The spectra were observed over a period of approximately one year, from 1 January 1963 to 12 February 1964.

Since the amount of water vapor within the slant path varied from day to day, it is difficult to determine the variation of transmission with zenith angle over the absorption band without further data reduction. To generate a composite plot which demonstrated this variation, each of the 41 curves were smoothed to a resolution of approximately 0.05 μ. The value of transmission vs. zenith angle was then plotted for each inflection point on the smoothed curves. These curves were used to generate the curves in Figure 9, which represent yearly averages

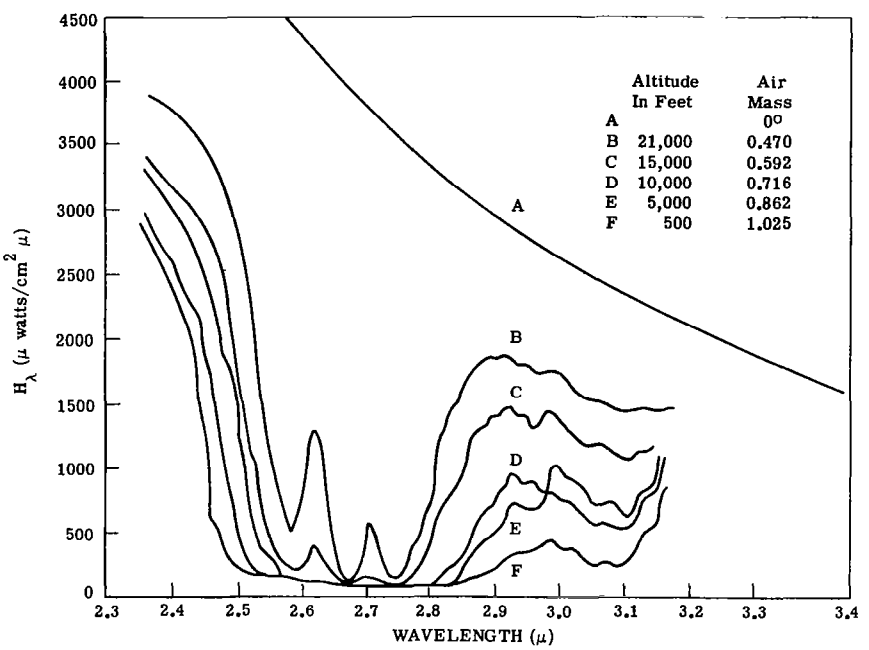

FIGURE 7. SOLAR SPECTRAL IRRADIANCE IN THE 2.8-μ REGION AT VARIOUS ALTITUDES (TEMPLIN) [6]

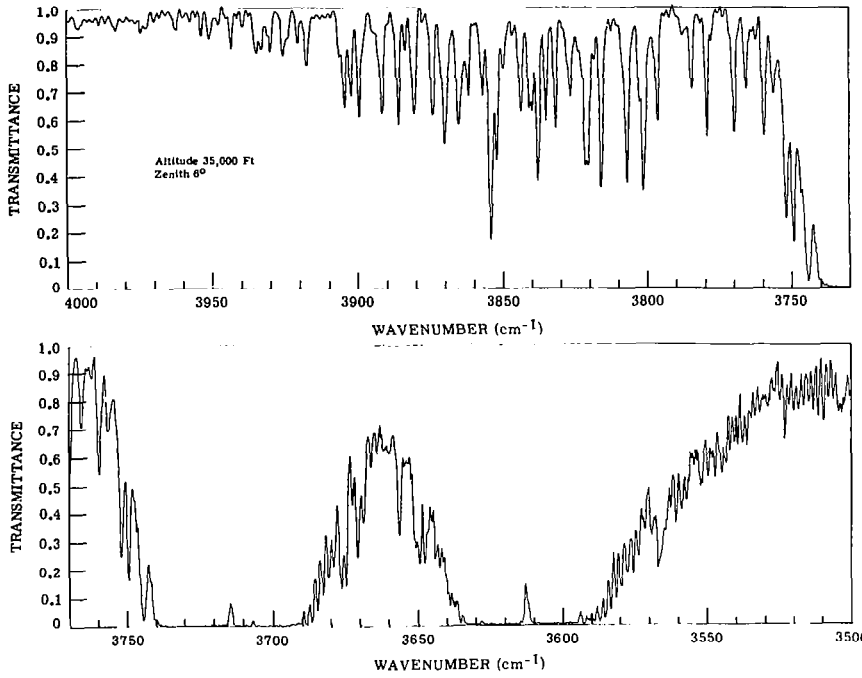

FIGURE 8. TRANSMITTANCE DETERMINED FROM SOLAR RADIATION MEASUREMENTS (CARDE)

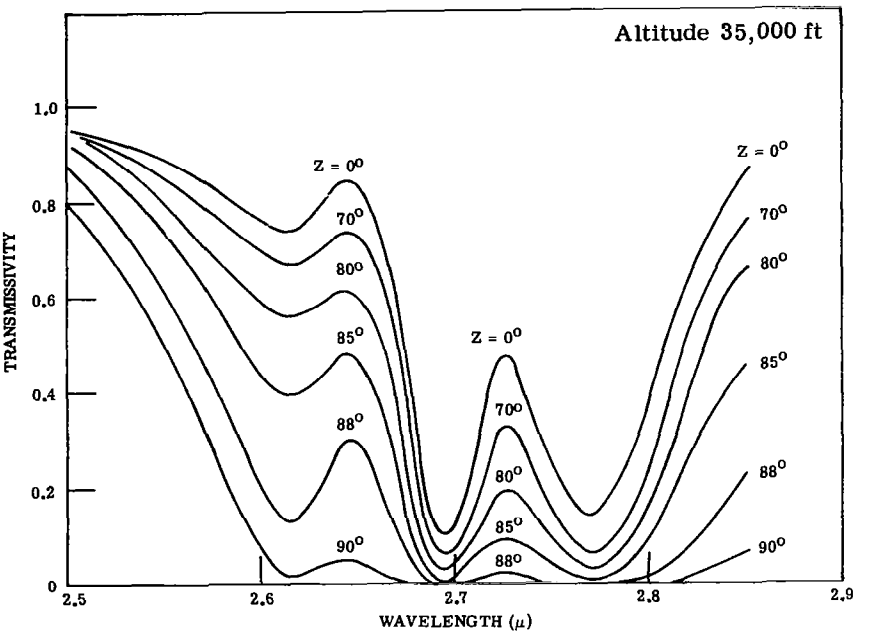

FIGURE 9. YEARLY AVERAGES OF TRANSMISSION VERSUS WAVELENGTH (CARDE)

of transmission for various zenith angles. The spectra obtained on any given day may vary from the average by plus or minus ten percentage points.

Since the majority of the work done by CARDE was confined to the absorption band rather than the window regions, it is presented here for completeness. They did obtain some measurements for the 2.85- to 3.35-μ wavelength region. These data are shown in figures 10-13. Since each curve represents a single measurement, variations in transmission with zenith, altitude, and water vapor content cannot be determined.

Murcray, Murcray, and Williams of the University of Denver have also been involved in high altitude solar spectra measurements for determining absolute transmission [15-20]. A prism spectrometer capable of scanning the 1.96- to 3.57-μ region was flown on a balloon launched from Holloman Air Force Base, New Mexico, on January 1963, obtaining solar spectra at various altitudes from ground through 23 km. A single pass Littrow prism spectrometer equipped with a LiF prism and a thermistor bolometer detector was used and the zenith measured with a biaxial pointing control. Figures 14 through 16 show the solar spectra reduced to transmission data. These three figures and table II represent all of the reduced data for this balloon flight. Because figure 15 contains so many curves, figure 17 reproduces a single curve, record 37, which, as an example of the Murcray findings, can be better examined out of context.

The University of Denver made further balloon flights in 1963 and 1964, but the complete set of data have not been reduced [21]. Spectra were obtained for the 2.7-, 4.3-, and 6.3-μ absorption bands. Figures 18, 19, and 20 are representative samples of the data taken at 4.3 μ. Each is compared with the spectra predicted by Plass who considered only CO_2 absorption, neglecting absorption by N_2O, which is a noticeable contributor in this region. Experimentalists at Denver stated that the uncertainty in the scale was sufficient to account for the spectral shift between the predicted and experimental curves. Data taken at altitudes near 35,000 ft were not published, but the figures indicate that absorption is complete at the center of the band to approximately 60,000 ft for a 50° zenith angle.

Bradley and Hampson of the Royal Radar Establishment (RRE) measured the solar spectra from a Canberra aircraft up to altitudes of 60,000 ft for the 4.3-μ absorption band [22]. Although their data were not reduced to absolute transmission spectra, their results indicated complete absorption up to 60,000 ft for zero zenith.

Henry Blau of the A. D. Little Corporation has been measuring the spectral-scattering properties of high altitude sunlit clouds in the 1.2- to 3.6-μ region [23]. During this program the spectrum of the sun was measured with the results shown in figures 21 and 22. Since the radiance values were not calibrated, only qualitative information can be determined from the spectra.

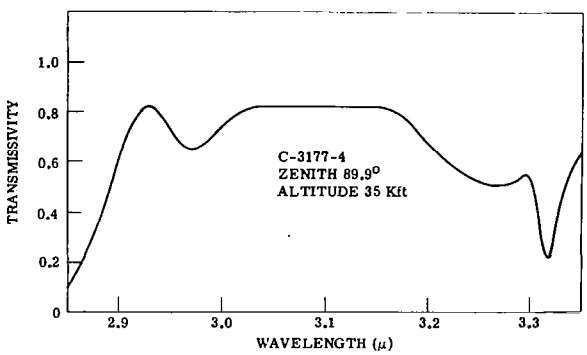

FIGURE 10. TRANSMISSION VERSUS WAVELENGTH (CARDE)

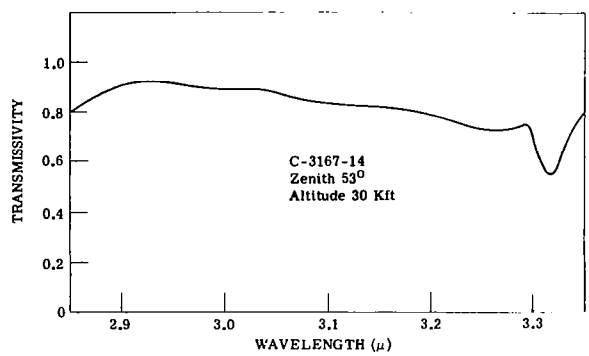

FIGURE 11. TRANSMISSION VERSUS WAVELENGTH (CARDE)

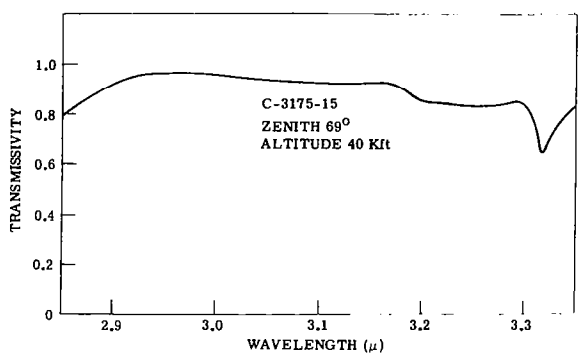

FIGURE 12. TRANSMISSION VERSUS WAVELENGTH (CARDE)

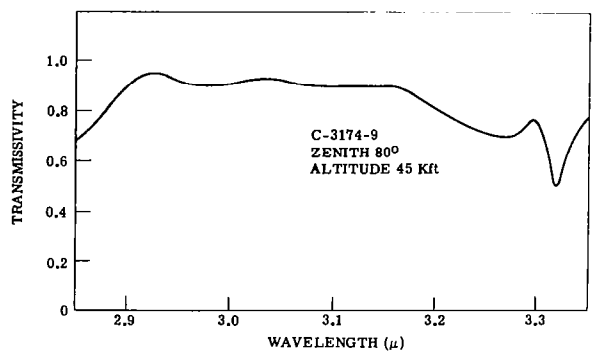

FIGURE 13. TRANSMISSION VERSUS WAVELENGTH (CARDE)

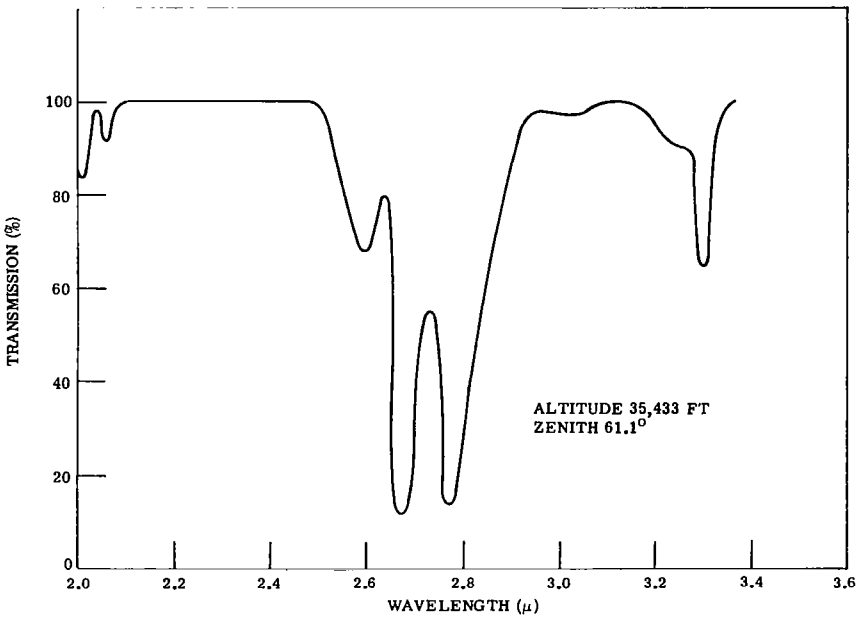

FIGURE 17. TRANSMISSION VERSUS WAVELENGTH (MURCRAY) [16]

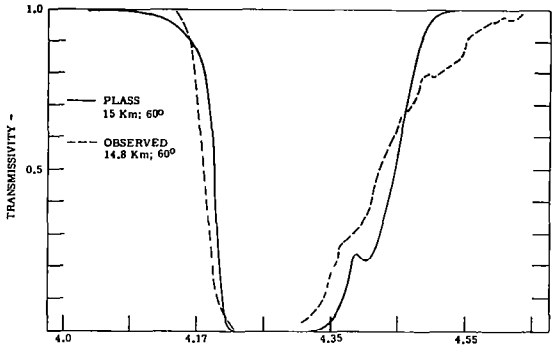

FIGURE 18. THEORETICAL AND OBSERVED SPECTRAL TRANSMISSION OF THE ATMOSPHERE AT 15 KM ALTITUDE FOR THE REGION FROM 4.0 μ to 4.65 μ (MURCRAY) [21]

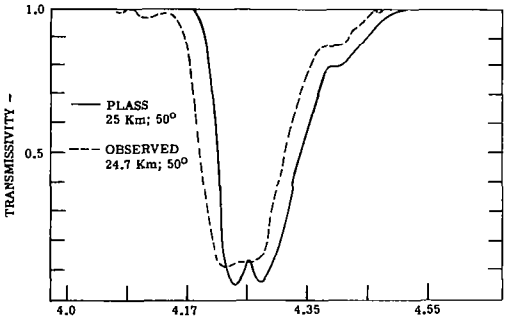

FIGURE 19. THEORETICAL AND OBSERVED SPECTRAL TRANSMISSION OF THE ATMOSPHERE AT 25 KM ALTITUDE FOR THE REGION FROM 4.0 μ TO 4.65 μ (MURCRAY) [21]

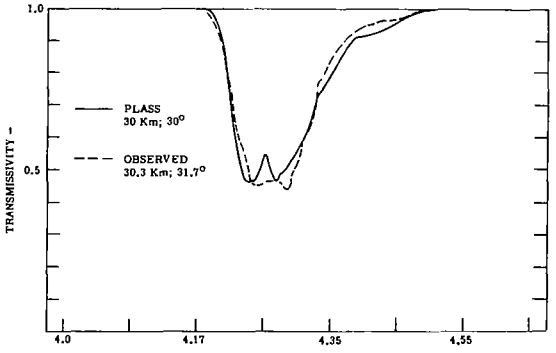

FIGURE 20. THEORETICAL AND OBSERVED SPECTRAL TRANSMISSION OF THE ATMOSPHERE AT 30 KM ALTITUDE FOR THE REGION FROM 4.0 μ TO 4.65 μ (MURCRAY) [21]

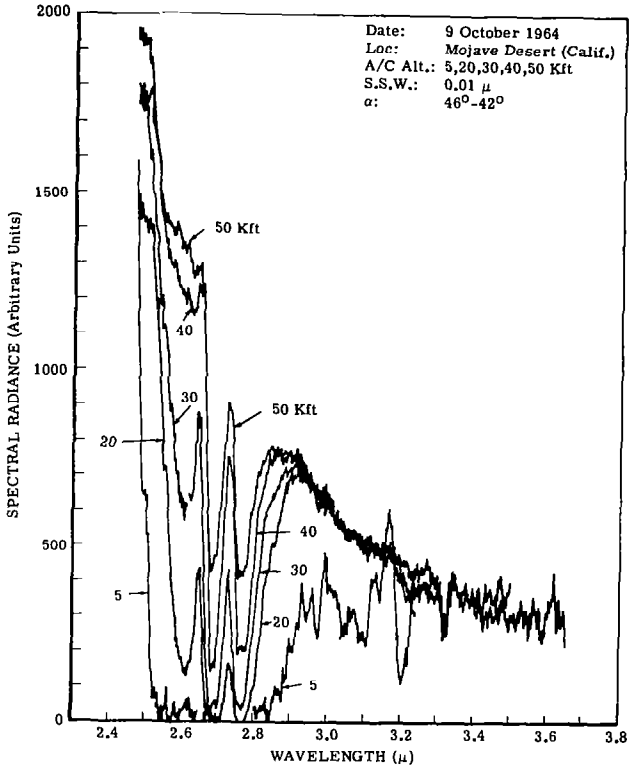

FIGURE 21. SOLAR SPECTRA: 2.4-3.6 μ (BLAU) [23]

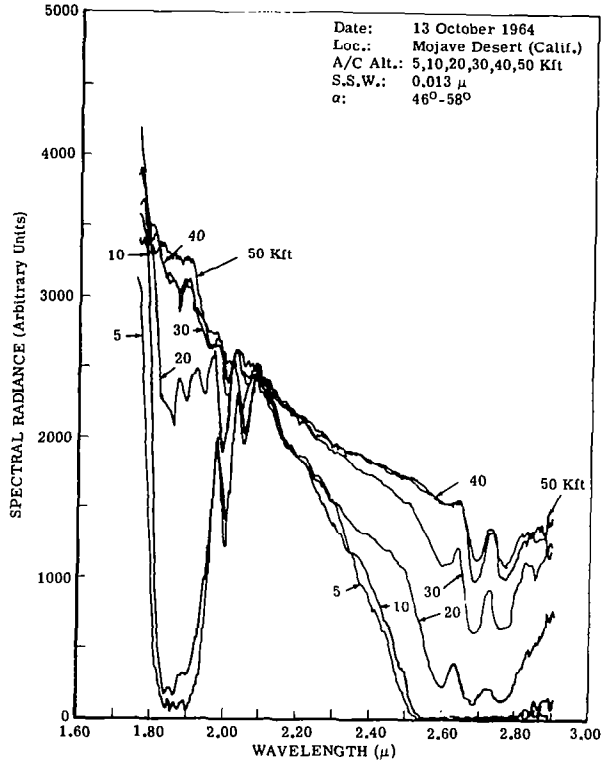

FIGURE 22. SOLAR SPECTRA: 1.7-2.9 μ (BLAU) [23]

An effort is being made by a group at The University of Michigan to reduce the data, but at present no results are available.

Farmer of EMI Electronics, England, made a survey of all available solar spectra for the 3.5- to 5.5-μ wavelength region and reduced selected data to absolute intensity with uniform resolution of approximately 0.015 μ [24]. His survey included spectra taken at altitudes ranging from sea level to 49,000 ft. Absolute transmission for 35,000 ft was determined by finding the difference between the spectra and the solar envelope and is shown in figure 23. By applying theoretical transmission functions and appropriate model atmospheres to the solar envelope used by Templin, Farmer also determined the absolute solar spectra for slant paths above 50,000 ft [25].

To present a composite view of the foregoing survey, a single curve (fig. 24) has been drawn that shows the average value of transmission spectra of the five contributors for azimuth angle of approximately 60° and an altitude of 35,000 ft. Because some groups did not make measurements over the entire 2- to 5-μ region, the wavelength interval is divided into five regions and the groups named in the regions where their data are used. No data are available beyond 4.5 μ, but Templin indicates in his work that the transmission is greater than 90% to 4.9 μ for an altitude of 17,000 ft. Thus for an altitude of 35,000 ft, it seems reasonable to assume that the transmission is nearly 100% to 4.9 μ. Changes in atmospheric conditions do cause changes in the spectrum presented, but it can be assumed on the basis of the data reviewed that such fluctuations will be less than 10 percentage points with the greatest effect in the absorption bands rather than in the window regions.

The summarized data indicate that the absorption is indeed very low in the various window regions, and this is probably the reason for the absence of extensive solar spectra for regions outside the absorption bands.

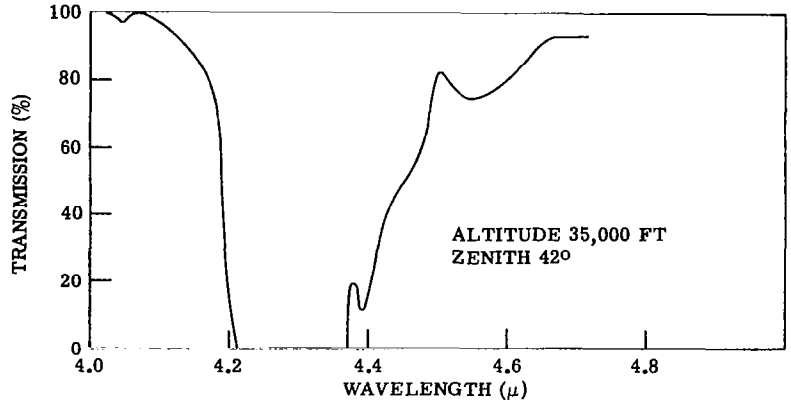

FIGURE 23. TRANSMISSION VERSUS WAVELENGTH DETERMINED FROM REDUCED SOLAR SPECTRA (FARMER) [24]

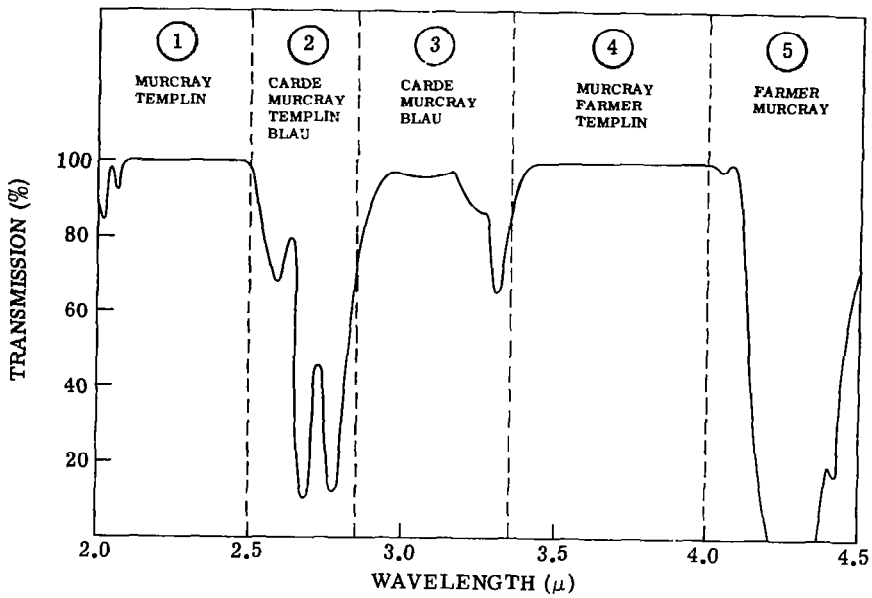

FIGURE 24. COMPOSITE TRANSMISSION SPECTRA

REFERENCES

1. Roy J. Nichols, Thomas W. Tuer, and William M. Hamilton, First Progress Report for Passive Infrared Acquisition and Tracking System Analysis, Task I: Surface and Flow-Field Radiation from Apollo Vehicle Reentry (U), Report No. 7399-12-P, Willow Run Laboratories, Institute of Science and Technology, The University of Michigan, Ann Arbor, to be published (CONFIDENTIAL).
2. Ely E. Bell et al., "Spectral Radiance of Sky and Terrain," J. Opt. Soc. Am., Vol. 50, 1960, p. 1313.
3. M. Migeotte, L. Neven, and J. Swensson, "The Solar Spectrum for 2.8 to 23.7 microns, Parts I and II," Mem. Soc. Roy. Sci. Liege, 1956.
4. O. C. Mohler et al., Photometric Atlas of the Near Infrared Solar Spectrum λ8465 to λ25242, University of Michigan Press, Ann Arbor, 1950.
5. J. T. Houghton et al., Phil. Trans. Roy. Soc. London, Ser. A., Vol. 254, No. 47, 1961.
6. H. A. Templin, Spectral Measurements of Solar Radiation from 2- to 5-μ up to 21,000 ft Altitude, 250600-5601, Naval Ordnance Laboratory, Corona, California, January 1956.
7. H. A. Templin, Proc. IRIS, Vol. 3, No. 4, 1958, p. 98.
8. F. Stauffer and J. Strong, Appl. Opt., Vol. 1, No. 2, March 1962, p. 129.
9. D. Markle, Project Lookout III: Stratospheric Infrared Transmission from Airborne Solar Spectra, Part I, T. M. 708/62, CARDE, Valcartier, Quebec, Canada, July 1962.
10. D. Markle, Project Lookout III: Solar Spectra Obtained January 12 to January 15, 1962, T. M. PCC-D-46-38-01-19, CARDE, Valcartier, Quebec, Canada, March 1962.
11. D. A. Markle, The Application of CARDE Solar Spectra to Determine Transmission Corrections for Radiometric Data, PCC-D-46-38-01-19, CARDE, Valcartier, Quebec, Canada, September 1962.
12. D. A. Markle et al., Project Lookout II: A Study of Launch Phase Ballistic Missile Radiation and of Atmospheric Transmission in the Infrared, T. M. 415/62, CARDE, Valcartier, Quebec, Canada, May 1962.
13. C. Cumming, J. Hampson, and R. P. Lowe, High Altitude Infrared Transmission Measurements, T. M. 288/59, CARDE, Valcartier, Quebec, Canada, November 1959.
14. C. Cumming and E. J. Fjarlie, Atmospheric Absorption Near Two Microns in the Solar Spectrum at 40,000 Feet, T. M. 246/59, CARDE, Valcartier, Quebec, Canada, April 1959.
15. David G. Murcray, Frank H. Murcray, and Walter J. Williams, Variation of Infrared Solar Spectrum with Altitude (Final Report), Report No. AFCRL TR 60-421, University of Denver, October 1960.
16. David G. Murcray et al., Instrumentation for Balloon-Borne Infrared Spectral Transmission Measurements of the Atmosphere, Report No. AFCRC-TN-60-264, University of Denver, February 1960.

REFERENCES (Continued)

17. David G. Murcray, James N. Brooks, and Norman J. Sible, Balloon Flight of January 29, 1962, Flight Data Report No. 3, Denver Research Institute, University of Denver, May 1962.

18. David G. Murcray, Frank H. Murcray, and Walter J. Williams, "Variation of the Infrared Solar Spectrum between 2800 and 5100 cm^{-1} with Altitude," J. Opt. Soc. Am., Vol. 54, January 1964.

19. David G. Murcray et al., Atmospheric Absorptions in the Near Infrared at High Altitudes, University of Denver, December 1958.

20. David G. Murcray et al., High Altitude Infrared Studies of the Atmosphere, Report No. AFCRC TN 57-295, University of Denver.

21. David G. Murcray et al., Infrared Atmospheric Transmittance and Flux Measurements (Six Month Technical Report No. 8), Report No. DRI 2168, University of Denver, July 1964.

22. J. Bradley and J. Hampson, Further Airborne Spectroscopic Measurements for Green Garland, RRE Memorandum No. 1068, Royal Radar Establishment, Malvern, England, October 1954, AD-72690.

23. Henry Blau, IR Spectral Properties of High Altitude Clouds (Final Report), A. D. Little Corporation, June 1965.

24. C. B. Farmer, Reduced Absolute Solar Spectra 3.5 to 5.5 microns, Part I: Altitude Range 0-50,000 ft., Report No. DP927, EMI Electronics Ltd., Hayes, England, 1961, AD-261 523.

25. C. B. Farmer, Reduced Absolute Solar Spectra 3.5 to 5.5 microns, Part II: Theoretical Spectra for Altitude Range 50,000 to 100,000 ft, EMI Electronics Ltd., Hayes, England, 1962, AD-287 053.